JACS
JOURNAL OF THE AMERICAN CHEMICAL SOCIETY
Article
pubs.acs.org/JACS

Theoretical Study of Exchange Coupling in 3d-Gd Complexes: Large Magnetocaloric Effect Systems

Eduard Cremades, Silvia Gómez-Coca, Daniel Aravena, Santiago Alvarez, and Eliseo Ruiz*

Departament de Química Inorgànica and Institut de Recerca de Química Teòrica i Computacional, Universitat de Barcelona, Diagonal 645, E-08028 Barcelona, Spain

Supporting Information

ABSTRACT: Polynuclear 3d transition metal-Gd complexes are good candidates to present large magnetocaloric effect. This effect is favored by the presence of weak ferromagnetic exchange interactions that have been investigated using methods based on Density Functional Theory. The first part of the study is devoted to dinuclear complexes, focusing on the nature and mechanism of such exchange interactions. The presence of two bridging ligands is found more favorable for ferromagnetic coupling than a triple-bridged assembly, especially for complexes with small M−O···O−Gd hinge angles. Our results show the crucial role of the Gd 5d orbitals in the exchange interaction while the 6s orbital seems to have a negligible participation. The analysis of the atomic and orbital spin populations reveals that the presence of spin density in the Gd 5d orbital is mainly due to a spin polarization effect, while a delocalization mechanism from the 3d orbitals of the transition metal can be ruled out. We propose a numerical DFT approach using pseudopotentials to calculate the exchange coupling constants in four polynuclear first-row transition metal-Gd complexes. Despite the complexity of the studied systems, the numerical approach gives coupling constants in excellent agreement with the available experimental data and, in conjunction with exact diagonalization methods (or Monte Carlo simulations), it makes it possible to obtain theoretical estimates of the entropy change due to the magnetization/demagnetization process of the molecule.

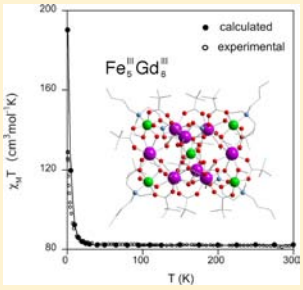

INTRODUCTION

Over the past few years many groups have focused their research on the search for new polynuclear complexes[1−3] combining 3d metals and lanthanides with potential applications, such as single-molecule magnets (SMMs)[4,5] or low-temperature magnetic refrigerants.[6−9] SMMs have been proposed as potential nanomagnets for high-density information storage devices.[10] Their application in magnetic refrigeration essentially exploits the entropy change in a magnetic material caused by its magnetization and the effect of removing the magnetic field. The spin polarization induced by the magnetic field reduces the degrees of freedom of the system, and when the field is switched off the magnetic contribution to the entropy becomes larger. If the demagnetization process is adiabatic, it leads to a drop in the temperature of the system.[7] This technology has been demonstrated to be more environment-friendly and more efficient than those based on a gas compression−expansion process.[6] This process has also received considerable attention, given the possibility of replacing the expensive helium-3 in ultra-low-temperature refrigeration.

The requirements for these two magnetic properties have some common features but also important differences:[8,11]

(i) In both cases a large total spin S is required. The main drawback for SMM is the lack of complexes with very high spin-flip energies in order to employ such systems as nanomagnets at room temperature. Thermal jump over the energy barrier or quantum tunneling can change the sign of the spin. Hence, the main challenge is to increase the energy barrier to avoid the spin-flip, given by $|D|\cdot S^2$, where S is the total spin of the molecule and D is the axial zero-field splitting parameter, that must be large and negative at least for integer spin systems. Also, for an ideal molecular refrigerant a large total spin S is needed because the magnetic entropy, neglecting low-lying excited state effects, is $R\ln(2S+1)$.

(ii) Concerning the magnetic anisotropy, there are opposite requirements, a large anisotropy for the SMMs, to get a high spin-flip barrier, but a negligible magnetic anisotropy for the molecular refrigerants that facilitates the polarization of the molecular spins using weak magnetic fields. Therefore, the magnetically isotropic f^7 configuration of the Gd^{III} cation makes it a perfect candidate for molecular refrigerants while other anisotropic lanthanide cations, e.g., Dy^{III}, Er^{III}, and Tb^{III}, are more appropriate for SMM behavior. Moreover, it is worth mentioning that a polynuclear Cu_8Gd_2 complex shows stronger SMM behavior (highest coercitivity) than the isomorphous complexes with Dy^{III} and Tb^{III} cations despite its lower anisotropy, thanks to the higher multiplicity of its ground state.[12]

(iii) The presence of low-lying excited states usually disturbs the SMM behavior due to mixing of states that enhances the undesired tunneling effects. In contrast, it increases the field-dependence of the magnetocaloric effect with a large number of populated spin states inducing a desired large entropy change. Thus, strong exchange interactions are welcome for SMMs, but a weak coupling is required for magnetic refrigerants.

(iv) The sign of the exchange interactions is crucial, since a ferromagnetic coupling favors a large S value that is convenient

Received: March 23, 2012
Published: May 25, 2012

   dx.doi.org/10.1021/ja302851n | J. Am. Chem. Soc. 2012, 134, 10532−10542

for both SMM and magnetic refrigerators. Antiferromagnetic interactions should be avoided because even in complexes with predominant ferromagnetic interactions leading to a ground state with the maximum possible total spin, the presence of excited states with lower S value will reduce the magnetocaloric effect. The analysis of the magnetic properties of compounds containing 4f ions is a difficult task since they usually present an important orbital contribution.[5,13] The exchange interactions are relatively weak due to the high degree of localization of the 4f orbitals. From the experimental point of view, the simultaneous presence of large magnetic anisotropy and weak exchange interactions makes it difficult to properly analyze the exchange coupling constants. However, the magnetically isotropic f^7 configuration of the Gd^{III} cation makes it a perfect case for studying the exchange interactions in systems bearing unpaired electrons in 3d and 4f orbitals, and to extend the conclusions to other lanthanides with large spin−orbit contributions.[14]

(v) Finally, for practical applications of the magnetocaloric effect it is also important to have a large metal/ligand mass ratio because the diamagnetic ligands do not contribute to such effect, while that feature is irrelevant for SMMs.

Only a few theoretical studies have undertaken the calculation of the magnetic properties in Gd^{III} dinuclear complexes with Cu^{II}, Ni^{II}, Fe^{II}, or Cr^{III} cations, using CASSCF/CASPT2[15,16] or DFT methods together with Slater or Gaussian basis sets.[17−20] The need of a very large active space for the former and the poor convergence and long computational times for DFT calculations have so far limited those studies to dinuclear complexes. Since many recent publications have been devoted to the synthesis and characterization of new 3d−4f polynuclear complexes, a theoretical tool that could help in the analysis of their magnetic properties would be desirable. For such systems, the use of hybrid DFT calculations with Gaussian basis sets could provide good results but is computationally very expensive.[21,22] Thus, this work has two main goals. First, we wish to analyze the mechanism of the exchange interaction between paramagnetic 3d transition metals and Gd^{III} cations that is crucial for SMMs and magnetic refrigerants. Our second goal is to check if fast methods based on the SIESTA code[23] using numerical basis sets with generalized gradient approximation (GGA) exchange-correlation functionals can provide a proper description of the magnetic interactions in polynuclear complexes in order to calculate the entropy change in those systems that can present magnetic refrigerant properties.

COMPUTATIONAL DETAILS

The calculated J values have been obtained using a non-projected approach.[21,22] For the dinuclear systems, the J value is proportional to the energy between high-spin (hs) state resulting from ferromagnetic coupling between the two paramagnetic centers and the low-spin (ls) solution for an antiferromagnetic coupling. In the case of the Heisenberg Hamiltonian,

$$\hat{H} = -J\hat{S}_1\cdot\hat{S}_2 \quad (1)$$

the J values can be obtained using the non-projected approach with the following expression:

$$J = \frac{E_{ls} - E_{hs}}{2S_1S_2 + S_2} \quad (2)$$

S_1 and S_2 being the local spin values. For polynuclear complexes, if the system has n different exchange pathways, we need to calculate the energy of at least $n + 1$ spin configurations (see Supporting Information) to extract the n coupling constants. The computer code employed for most of the calculations is the program SIESTA[23] (Spanish Initiative for Electronic Simulations with Thousands of Atoms). This code has been developed and designed for efficient calculations in large low-symmetry systems. We have employed the generalized-gradient functional proposed by Perdew, Burke, and Erzernhof.[24] Only valence electrons are included in the calculations, with the core being replaced by norm-conserving scalar relativistic pseudopotentials factorized in the Kleinman−Bylander form.[25] The pseudopotentials are generated according to the procedure of Troullier and Martins.[26] We have used a Gd pseudopotential proposed by Pollet et al. which has been tested with the PBE functional and has been shown to be as accurate as the CCSD(T) methodology in the study of Gd^{III} solvate compounds as magnetic resonance imaging agents.[27] For the Mn atoms we have employed a pseudopotential including the 3s and 3p orbitals in the basis set, which has been previously tested to give accurate J values,[21] while for Fe and Cu atoms the pseudopotential has a larger core, also including such orbitals. We have also employed a numerical basis set of triple-ζ quality for the transition metal atoms and a double-ζ one with polarization functions for the main-group elements. There are two parameters that control the accuracy of these numerical calculations: (i) since the wave function vanishes at the chosen confinement radius r_c, whose value is different for each atomic orbital, the energy radii of different orbitals are determined by a single parameter, *the energy shift*, which is the energy increase of the atomic eigenstate due to the confinement; and (ii) the integrals of the self-consistent terms are obtained with the help of a regular real-space grid onto which the electron density is projected. The grid spacing is determined by the *maximum kinetic energy* of the plane waves that can be represented in that grid. We have studied the influence of these two parameters on the calculated J value for 3d systems[21] and found that the values of 50 meV for the energy shift and 250 Ry for the mesh cutoff provide a good compromise between accuracy and computer time required to estimate the exchange coupling constants.

The calculations of dinuclear complexes using a Gaussian basis set were performed with the Gaussian09 code employing the hybrid B3LYP functional and the DKH method to introduce scalar relativistic effects.[28] We used for all elements the triple-ζ basis set proposed by Schäfer et al.,[29] with the exception of Gd, for which we adopted an all-electron basis set with a contraction pattern (10 555311/86631/6421/411) obtained from an uncontracted basis set proposed by Nakajima et al.[30] The contraction of this basis set is slightly modified in comparison with the one previously employed in order to facilitate the elimination of the functions corresponding to the 5d and 6s orbitals.[18,19] In spite of the smaller basis set, the calculated J value for the studied $Cu^{II}Gd^{III}$ complex remains very similar.

RESULTS AND DISCUSSION

Exchange Interactions in Dinuclear 3d-Gd Complexes.

Most of the published theoretical work on transition metal−lanthanide systems using DFT methods has been devoted to Cu^{II}−Gd^{III} complexes.[18,19] One of the most debated features of these systems is the role of the "empty" Gd orbitals in the exchange interactions since the $4f^7$ orbitals of Gd are contracted around the nucleus and they are efficiently shielded by the 5s and 5p occupied orbitals. Two possible different mechanisms have been proposed. Kahn et al.[31,32] suggested that the 3d orbitals of the Cu atoms can transfer electron density to the empty Gd 5d orbitals, while Gatteschi et al.[33,34] proposed a spin polarization mechanism involving the interaction of the tails of the Cu 3d orbitals with the empty Gd 6s orbital. Despite the different terminology used, both proposals imply the participation of the Cu 3d orbitals in the exchange coupling, essentially differing only in the empty orbitals of the gadolinium atoms (6s or 5d) involved in the exchange mechanism. Previously, Paulovic et al.[16] suggested from CASSCF calculations that the Gd 5d orbitals should be included in the active space to reproduce the experimental J values, since they should play a key role in the exchange interaction. Also, Rajaraman et al. suggested that the 5d orbitals should be considered to explain the

dx.doi.org/10.1021/ja302851n | J. Am. Chem. Soc. 2012, 134, 10532−10542

Table 1. Structural and Magnetic Data for Alkoxo-Bridged (μ_2-OR)M−Gd^{III} Complexes, Where M Is a Non-copper Paramagnetic 3d Cation[a]

complex	CSD refcode	ref	M···Gd	no. of Bridges	M−O···O−Gd	M−O−Gd	J
$[LNi^{II}(H_2O)_2Gd](NO_3)_3$	NOJLON	36	3.521	2	3.1	106.5, 107.9	+3.6
$[LNi^{II}Gd(EtOH)_2](EtOH)_2$	TAKGOD	37	3.482	2	2.6	106.0, 106.1	+0.7
$[LNi^{II}Gd(hfac)_2](EtOH)$	IYEQUY	38	3.170	3	52.3	89.9, 90.8, 91.7	+0.7
$[LNi^{II}Gd(DMF)](ClO_4)_2$	UDUYIB	39	3.210	3	51.4	90.2, 92.3, 94.3	+0.6
$[LNi^{II}Gd](ClO_4)_2$	KAJKEN	14	2.988	3	57.0	85.4, 85.7, 85.9	−0.2
$LCo^{II}(MeOH)Gd(NO_3)_3$	HUNVER	40	3.531	2	4.2	106.5, 109.1	+0.9
$[LFe^{II}(MeOH)Gd(NO_3)_3](MeOH)$	MOGTOR	35	3.506	2	6.2	106.3, 107.3	+1.0
$[LFe^{II}((CH_3)_2CO)Gd](NO_3)_3$	MOGTUX	35	3.517	2	23.6	105.2, 105.5	+0.8
$[LFe^{II}((CH_3)_2CO)Gd](NO_3)_3$	MOGVAF	35	3.415	2	24.1	103.5, 103.6	+0.2
$[LMn^{II}Gd](ClO_4)_2$	KAJKIR	14	3.125	3	55.4	86.9, 87.7, 88.3	−1.7
$[LV^{IV}(O)Gd(H_2O)](NO_3)_3$	QEYXOH	41	3.519	2	3.5	107.1, 108.8	+1.5
$[LV^{IV}(O)((CH_3)_2CO)Gd](NO_3)_3$	QEYXUN	41	3.504	2	20.7	105.1, 105.4	−2.6

[a]See ref 18 for Cu^{II}−Gd^{III} complexes. Average distances, angles, and J values are in Å, degrees, and cm^{-1} respectively, and L represents any of a variety of multidentate ligands.

interaction mechanism, because they are important for the exchange interaction through spin delocalization from both the 4f orbitals of the Gd^{III} cation and the 3d orbitals of the Cu^{II} centers.[19] A similar study on Gd^{III}−Ni^{II} complexes was recently published by Singh et al.[20]

In order to extend our study of the magnetic properties to other dinuclear complexes with more unpaired electrons (see Table 1) and, consequently, more suitable for SMM and magnetic refrigerant properties, we have selected two dinuclear $Mn^{II}Gd^{III}$ and $Fe^{II}Gd^{III}$ complexes, one showing an antiferromagnetic coupling through three alkoxo bridging ligands, $[Mn^{II}Gd^{III}\{pyCO(OEt)pyC(OH)(OEt)py\}_3](ClO_4)_2$ (**1**, CSD refcode KAJKIR),[14] and the second one with ferromagnetic coupling through two phenoxo bridging ligands, $[Fe^{II}Gd^{III}L(MeOH)(NO_3)_3]$ (**2**, CSD refcode MOGTOR),[35] where H_2L = *N*,*N*′-bis(3-methoxysalicylidene)-1,3-diamino-2,2′-dimethylpropane (Figure 1). The experimental J values are −1.7 and +1.0 cm^{-1}

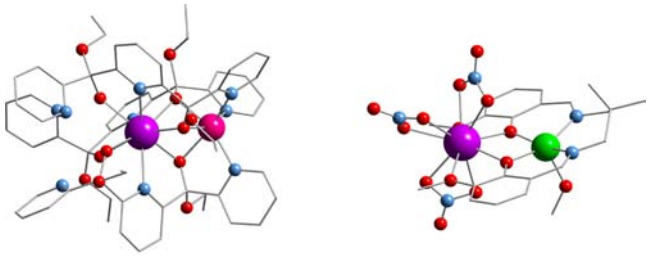

Figure 1. Studied dinuclear complexes, $[Mn^{II}Gd^{III}\{pyCO(OEt)pyC(OH)(OEt)py\}_3](ClO_4)_2$ (**1**)[14] and $[Fe^{II}Gd^{III}L(CH_3OH)(NO_3)_3]$ (**2**, H_2L = *N*,*N*′-bis(3-mehoxysalicylidene)-1,3-diamino-2,2′-dimethylpropane).[35] Violet, pink, green, red, and blue spheres are for gadolinium, manganese, iron, oxygen, and nitrogen atoms, respectively. The carbon atoms are represented using a wire framework.

for **1** and **2**, respectively, while the calculated ones using numerical PBE calculations with the SIESTA code are −2.7 and +1.4 cm^{-1}, respectively. Hence the employed DFT methodology seems to correctly reproduce both J values, as in the case of $Cu^{II}Gd^{III}$ complexes using Gaussian basis sets and hybrid functionals.[18]

The analysis of the experimental J values in Table 1 seems to indicate that the presence of two bridging ligands (edge sharing complexes) favors a stronger ferromagnetic coupling, especially for complexes with small M−O···O−Gd hinge angles (defined as 180° − M−O···O−Gd torsion angle). To corroborate this fact, we have repeated the calculations for the $Fe^{II}Gd^{III}$ complex **2** with a hinge angle of 6.2° (see Table 1, calculated J value of +1.4 cm^{-1}) using two new Fe−O···O−Gd hinge angles of 20 and 40°, that result in J values of +1.1 and +0.3 cm^{-1}, respectively. These results show the same trend that was obtained previously for the $Cu^{II}Gd^{III}$ complexes,[18] with larger deviations of the M(μ-O)$_2$Gd core from planarity implying an enhanced antiferromagnetic coupling.

For the complexes with three bridging ligands (face-sharing complexes), we have analyzed the dependence of the J value on the M−O···O−Gd hinge angle and/or the M−O-Gd bond angle using a model structure of the $Mn^{II}Gd^{III}$ complex, replacing the N and O ligands by ammonia and water (or OH^- for bridging ligands) to allow the building of distorted models with varying M−O···O−Gd angles and the same metal−ligand distances. It is worth mentioning that in the models a change in the M−O···O−Gd hinge angle always implies a change in the M−O−Gd bond angle, since these two geometric parameters are not independent. The calculated J value for the model structure is −2.9 cm^{-1}, relatively close to the value of the complex with the whole ligands (−2.7 cm^{-1}). The dependence of the calculated coupling constant on the M−O···O−Gd angle is represented in Figure 2. The variation shows a qualitative behavior similar to that of the systems with two bridging ligands (edge sharing complexes); a larger hinge M−O···O−Gd angle increases the antiferromagnetic contribution. Due to the structure of the face-sharing complexes, they always have larger hinge M−O···O−Gd angles than the edge-sharing complexes and larger antiferromagnetic contributions.

In order to analyze in detail the mechanism of the 3d-Gd^{III} exchange interaction, we have selected three systems, a Cu^{II}−Gd^{III} complex previously studied[18] and the $Mn^{II}Gd^{III}$ and $Fe^{II}Gd^{III}$ complexes **1** and **2** mentioned above, to consider cases with more than one unpaired electron in the 3d metal and a different nature of the exchange interactions. The calculations for such systems were performed with the Gaussian09 code because it is easier to control the basis set than in the SIESTA calculations (see Computational Details section). The calculated exchange coupling constants, collected in Table 2, reproduce well the antiferromagnetic and ferromagnetic nature of the coupling in the $Mn^{II}Gd^{III}$ and $Fe^{II}Gd^{III}$ complexes, similarly to the results obtained with the SIESTA code mentioned above. To analyze

dx.doi.org/10.1021/ja302851n | J. Am. Chem. Soc. 2012, 134, 10532−10542

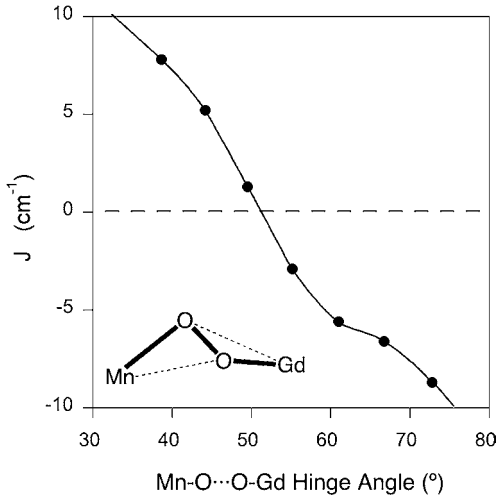

Figure 2. Dependence of the calculated J value (SIESTA calculations) on the Mn−O···O−Gd hinge angle for a model structure of a $Mn^{II}Gd^{III}$ complex **1** (CSD refcode KAJKIR) in which the N- and O-donor ligands have been replaced by ammonia, water, and OH^-.

the exchange mechanism, three types of calculations were performed, using the full basis set or omitting two s or two sets of d functions of the gadolinium atoms. Thus, in the second case only five s functions are employed and, consequently, the 6s orbital is not included, while deletion of two d function sets leaves us with only two d sets that describe the Gd 3d and 4d atomic orbitals. Although the 6s and 5d electron populations have similar occupations, the presence of the 5d functions in the basis set is crucial to properly reproduce the experimental ferromagnetic J value, whereas the elimination of the 6s orbital from the basis set does not significantly affect the calculated J values. This difference is probably associated with the presence of a non-negligible spin population in the Gd 5d orbitals.[35]

The most surprising results come from the analysis of the atomic and spin populations of the ls solutions that correspond to an opposite alignment of the spins of the Gd and 3d metal centers. The values are practically identical to those of the hs state (parallel alignment) shown in Table 2, except for the obvious difference in the sign of the spin population at the 3d metal. This fact is remarkable because with the previously proposed mechanisms[19] the inversion of the sign of the spin density of the 3d metal should be reflected in the sign of the Gd^{III} 5d spin population. For instance, for the $Cu^{II}Gd^{III}$ complex, the 5d population in the ls configuration is reduced by only 0.004 e^- from the hs one (see Table 2), consistent with a very small delocalization of the Cu 3d electrons onto the Gd 5d orbitals. In order to further verify our conclusion about the "non-influence" of the 3d metal on the magnetic features of the Gd^{III} centers, we performed a calculation for a Cu^{II}−Gd^{III} model in which the Cu^{II} center was removed from the complex. The results (Table 2) show that the spin populations are very similar to those of the binuclear system, indicating that the spin population in the Gd 5d orbitals is practically unaffected by the presence of the 3d metal electrons. We can conclude that the positive spin populations at the Gd 5d orbitals can only be due to the influence of the Gd 4f orbitals through one of two possible mechanisms: (a) a 5d−4f mixing at Gd or (b) the spin polarization of the Gd−ligand bonding electron pairs involving the formally empty 5d orbitals.

In order to rule out one of these two mechanisms, we carried out calculations for an octahedral $[GdCl_6]^{3-}$ model, for which the f orbitals ($T_{1u}+T_{2u}+A_{2u}$ representation) are forbidden by symmetry to mix with the d orbitals ($T_{2g}+E_g$). A NBO analysis of the spin population for this anion still returns a positive spin population (0.042 e^-) in the 5d orbitals that can only be due to spin polarization. The negative spin populations at the atoms coordinated to the Gd^{III} cations is another manifestation of the spin polarization of the Gd−ligand bonding electron pairs.[18] In a spin polarization mechanism, the exchange energy is optimized by having spin of the same sign in all atomic orbitals of the Gd atom[44] and the opposite sign at the coordinated donor atoms.[18]

The results for the $Mn^{II}Gd^{III}$ and $Fe^{II}Gd^{III}$ complexes **1** and **2**, with more than one 3d unpaired electron, follow essentially the same trend than those of the Cu^{II} complex. Thus, the presence of Gd 5d orbitals is vital to reproduce the experimental exchange

Table 2. Calculated J Values (cm^{-1}) Together with Natural Bond Orbital (NBO)[43] Atomic and Spin Populations (in Parentheses) Obtained Using the B3LYP Functional and a Gaussian Basis Set for the High-Spin (hs) or Low-Spin (ls) Wave Functions of a Previously Studied Cu^{II}−Gd^{III} System[42] and Two 3d M−Gd^{III} Complexes, $Mn^{II}Gd^{III}$ (1)[14] and $Fe^{II}Gd^{III}$ (2)[35]

basis set[a]	J	4f (Gd)	5d (Gd)	6s (Gd)	3d (M)
		Cu^{II}−Gd^{III}, J_{exp} = +10.1 cm^{-1}			
hs, full basis set	+9.6	7.33 (6.67)	0.18 (0.029)	0.11 (0.00)	9.36 (0.56)
hs, no Gd 5d orbitals	−0.9	7.45 (6.54)		0.12 (0.00)	9.35 (0.57)
hs, no Gd 6s orbitals[b]	+10.2				
without Cu^{II}		7.10 (6.88)	0.23 (0.035)	0.10 (−0.01)	
ls, full basis set		7.32 (6.67)	0.19 (0.025)	0.09 (0.00)	9.36 (−0.53)
		1 Mn^{II}−Gd^{III}, J_{exp} = −1.7 cm^{-1}			
hs, full basis set	−3.2	7.08 (6.90)	0.17 (0.023)	0.13 (0.00)	5.22 (4.66)
hs, no Gd 5d orbitals	−4.8	7.12 (6.86)		0.14 (0.00)	5.23 (4.66)
hs, no Gd 6s orbitals[b]	−3.3				
ls, full basis set		7.08 (6.90)	0.17 (0.024)	0.13 (0.00)	5.22 (−4.66)
		2 Fe^{II}−Gd^{III}, J_{exp} = +1.0 cm^{-1}			
hs, full basis set	+0.11	7.09 (6.89)	0.22 (0.029)	0.13 (0.00)	6.21 (3.70)
hs, no Gd 5d orbitals	−1.65	7.16 (6.82)		0.14 (0.00)	6.21 (3.70)
hs, no Gd 6s orbitals[b]	+0.14				
ls, full basis set		7.10 (6.89)	0.22 (0.027)	0.13 (0.00)	6.21 (−3.70)

[a]In order to check the influence of the Gd orbitals on the calculated J value, we repeated the ls and hs calculations eliminating some functions (without 5d or 6s orbitals). [b]NBO analysis could not be performed in the absence of valence Gd 6s functions.

dx.doi.org/10.1021/ja302851n | J. Am. Chem. Soc. 2012, 134, 10532−10542

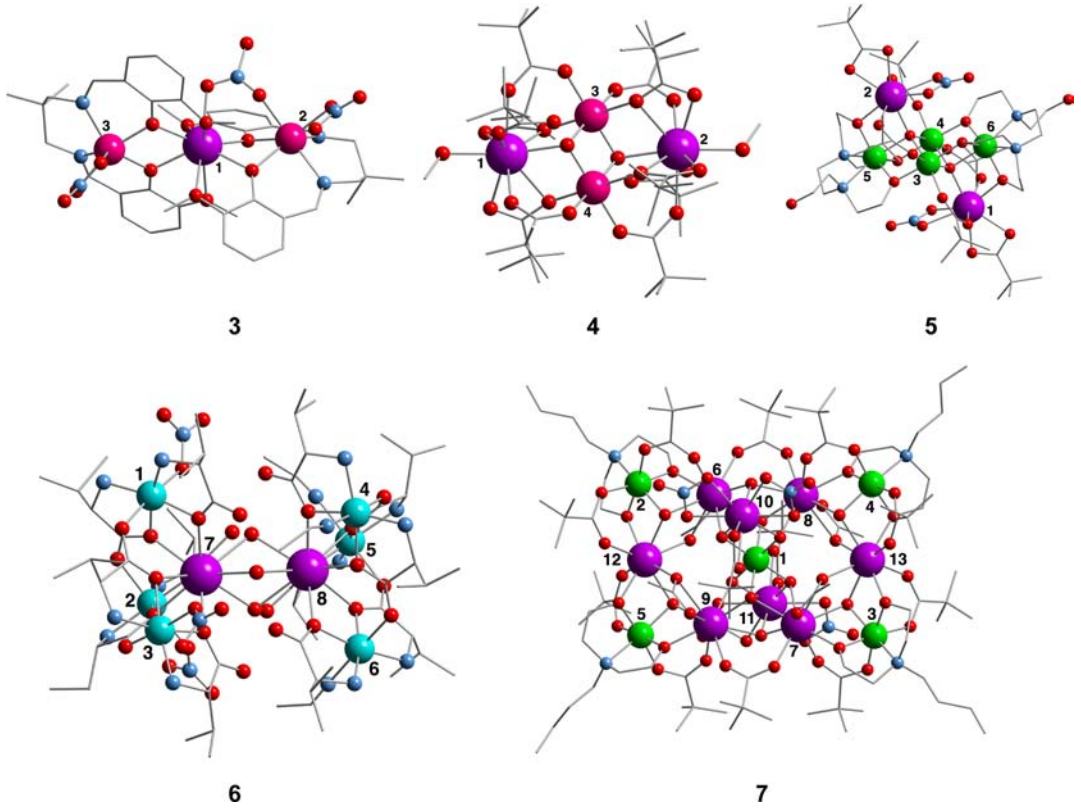

Figure 3. Studied first-row transition metal−Gd^{III} polynuclear complexes $[(NO_3)Mn^{II}(L)(\mu\text{-}NO_3)Gd^{III}(L)Mn^{II}(NO_3)]$ (**3**),[45] $[Mn^{III}_2Gd^{III}_2O_2(O_2CCMe)_8(HO_2CCMe_3)_2(MeOH)_2]$ (**4**),[46] $[Fe^{III}_4Gd^{III}_2(\mu_4\text{-}O)_2(NO_3)_2(piv)_6(Hedte)_2]$ (**5**)[47] $[Et_4N][Ni^{III}_6Gd^{III}_2(val)_{12}(MeCN)_6(H_2O)_3][Gd(NO_3)_5](ClO_4)_5$ (**6**),[8] and $[Fe^{III}_5Gd^{III}_8(\mu_3\text{-}OH)_{12}(L)_4(piv)_{12}(NO_3)_4(OAc)_4](H_3L)$ (**7**).[48] Violet, pink, green, light blue, red, and blue spheres represent gadolinium, manganese, iron, nickel, oxygen, and nitrogen atoms, respectively. The carbon atoms are represented using a wire framework.

coupling constants, and the hs and ls wave functions have similar positive spin density populations in the Gd 5d orbitals regardless of the number of unpaired electrons in the 3d cation (see Table 2). This feature clearly shows the irrelevance of the spin transfer from the 3d orbitals of the Mn^{II} or Fe^{III} cations to the Gd 5d orbitals and the predominance of the spin polarization mechanism.

Magnetic Properties of Polynuclear 3d-Gd Complexes. In this section, we wish to extend our study to the calculation of the exchange coupling constants in medium- and large-sized 3d metal−Gd^{III} polynuclear complexes. As discussed in the Introduction, the presence of ferromagnetic interactions is crucial for the ability of such systems to act as magnetic refrigerants. To that end we have selected five complexes represented in Figure 3: a trinuclear complex $[(NO_3)Mn^{II}(L)(\mu\text{-}NO_3)Gd^{III}(L)Mn^{II}(NO_3)]$, where L is a Schiff base ligand (H_2L = *N*,*N*′-2,2-dimethylpropylenebis(3-methoxysalicylideneimine), refcode LUDCIX, **3**);[45] a butterfly tetranuclear complex $[Mn^{III}_2Gd^{III}_2O_2(O_2CCMe)_8(HO_2CCMe_3)_2(MeOH)_2]$ (refcode DIMVIE, **4**);[46] the hexanuclear complex $[Fe^{III}_4Gd^{III}_2(\mu_4\text{-}O)_2(NO_3)_2(piv)_6(Hedte)_2]$ (H_4edte = *N*,*N*,*N*′,*N*′-tetrakis(2-hydroxyethyl)ethylenediamine, refcode GUMJEE, **5**);[47] an octanuclear complex showing appealing properties as a magnetic cooler, $[Et_4N][Ni^{III}_6Gd^{III}_2(val)_{12}(MeCN)_6(H_2O)_3][Gd(NO_3)_5](ClO_4)_5$ (val = valine anion, refcode EXEFET **6**);[8] and the tridecanuclear complex $[Fe^{III}_5Gd^{III}_8(\mu_3\text{-}OH)_{12}(L)_4(piv)_{12}(NO_3)_4(OAc)_4](H_3L)$ (H_2 L = *N*-butyldiethanolamine, refcode QISKAF, **7**).[48]

For large 3d-Gd polynuclear complexes with more than six paramagnetic centers it is not possible to extract the exchange coupling constants by fitting the experimental magnetic susceptibility data, due to the large size of the Hamiltonian matrix. Thus, we have selected the three small polynuclear complexes, in order to check the accuracy of the calculated *J* values in comparison with the experimental data. One of the largest systems, **6**, corresponds to a molecule that has been proposed as a magnetic cooler,[8] and it will allow us to check the ability of the employed theoretical methodology to estimate the magnetic entropy change. In order to analyze the magnetic properties, the spin Hamiltonians indicated in eqs 3−7 have been employed for complexes **3**−**7**, respectively.

$$\hat{H} = -J_1\hat{S}_1\hat{S}_2 - J_2\hat{S}_1\hat{S}_3 \tag{3}$$

$$\hat{H} = -J_1\hat{S}_3\hat{S}_4 - J_2[\hat{S}_1\hat{S}_3 + \hat{S}_2\hat{S}_4] - J_3[\hat{S}_1\hat{S}_4 + \hat{S}_2\hat{S}_3] - J_4\hat{S}_1\hat{S}_2 \tag{4}$$

$$\hat{H} = -J_1\hat{S}_3\hat{S}_4 - J_2[\hat{S}_3\hat{S}_5 + \hat{S}_4\hat{S}_6] - J_3[\hat{S}_3\hat{S}_6 + \hat{S}_4\hat{S}_5] - J_4[\hat{S}_1\hat{S}_3 + \hat{S}_2\hat{S}_4] - J_5[\hat{S}_1\hat{S}_4 + \hat{S}_2\hat{S}_3] - J_6[\hat{S}_1\hat{S}_6 + \hat{S}_2\hat{S}_5] \tag{5}$$

$$\hat{H} = -J_1[\hat{S}_1\hat{S}_2 + \hat{S}_1\hat{S}_3 + \hat{S}_2\hat{S}_3 + \hat{S}_4\hat{S}_5 + \hat{S}_5\hat{S}_6 + \hat{S}_4\hat{S}_6] - J_2[\hat{S}_1\hat{S}_7 + \hat{S}_2\hat{S}_7 + \hat{S}_3\hat{S}_7 + \hat{S}_4\hat{S}_8 + \hat{S}_5\hat{S}_8 + \hat{S}_6\hat{S}_8] - J_3\hat{S}_7\hat{S}_8 \tag{6}$$

dx.doi.org/10.1021/ja302851n | *J. Am. Chem. Soc.* 2012, 134, 10532−10542

Table 3. Structural and Magnetic Data for the Studied Polynuclear 3d-Gd^{III} Complexes 3−7 (See Figure 3)[a]

				J	
interaction	bridging ligands	M···M	M−O···O−Gd	expt	calc
		$Mn^{II}_2Gd^{III}$ (3)			
J_1 Mn···Gd	2(μ_2-OR)(μ-NO_3)	3.515	39.9	+0.0	−0.2
J_2 Mn···Gd	2(μ_2-OR)	3.709	3.3	+1.6	+1.9
		$Mn^{III}_2Gd^{III}_2$ (4)			
J_1 Mn···Mn	2(μ_3-O)	2.868		−62.9	−67.2
J_2 Mn···Gd	(μ_3-O)(μ_2-OCMe)	3.471	18.5	+2.4[b]	+1.2
J_3 Mn···Gd	(μ_3-O)(μ_2-OCMe)	3.466	19.6		+1.5
J_4 Gd···Gd	Mn_2O_2	6.317		−0.01	−0.04
		$Fe^{III}_4Gd^{III}_2$ (5)			
J_1 Fe···Fe	2(μ_4-O)	3.018		+3.2	+0.4
J_2 Fe···Fe	(μ_4-O)(μ_2-OR)	3.172		−8.8[b]	−13.8
J_3 Fe···Fe	(μ_4-O)(μ_2-OR)	3.101			−5.8
J_4 Fe···Gd	(μ_4-O)(μ-O_2CMe)	3.879		+0.5[c]	−1.2
J_5 Fe···Gd	(μ_4-O)(μ-O_2CMe)	3.780			−1.1
J_6 Fe···Gd	(μ_4-O)(μ_2-OR)	3.442	10.5	−0.2	+1.0
		$Ni^{II}_6Gd^{III}_2$·Gd^{III}(6)			
J_1 Ni···Ni	(μ-O_2CR)	5.310		−4.3	−1.2
J_2 Ni···Gd	(μ_2-OR)(μ_2-OCOR)	3.516	10.1	+0.86	+1.4
J_3 Gd···Gd	3(μ_2-OH_2)	3.887	43.8	+0.14	+0.02
		$Fe^{III}_5Gd^{III}_8$ (7)			
J_1 Gd···Gd	2(μ_3-OH)(μ-O_2CMe)	3.970	29.6		+0.4
J_2 Gd···Gd	(μ_3-OH)(μ_2-O_2CMe)	4.237	6.2		+0.1
J_3 Gd···Gd	2(μ_3-OH)	3.901	25.6		−0.05
J_4 Fe···Gd	2(μ_3-OH)	3.498, 3.520	15.7, 16.9		+0.4
J_5 Fe···Gd	(μ_3-OH)(μ-O_2CMe) (μ_2-OR)	3.389, 3.427	15.6, 14.8		−0.6

[a]Average distances, angles, and J values are in Å, degrees, and cm^{-1} respectively. The calculated values for complex **6** were reported previously.[8] [b]J_2 and J_3 considered equivalent in the experimental study. [c]J_4 and J_5 considered equivalent in the experimental study.

Table 4. Structural Data for Trinuclear 3d-Gd^{III}-3d Complexes (for Magnetic 3d Cations) Together with the Experimental J Values[a]

complex	CSD refcode	ref	M···Gd	bridging ligands	M−O···O−Gd	J_{exp}
$[Cu_2GdL_4(NO_3)(H_2O)_2](ClO_4)(NO_3)$	XAYTOH	10	3.367, 3.368	2(μ_2-OR)	4.4, 2.4	+5.8
$[(L_2Cu)_2Gd(H_2O_3)](ClO_4)_3$	DITGOC	50	3.367	2(μ_2-OR)	16.6	+5.3
$[Cu_2GdL_2(NO_3)_3(dmf)_2]$[b]	NAFDII	51	3.608, 3.681	2(μ_2-OR)	14.4, 7.2	+2.8
$[(L_2Cu)_2Gd(H_2O)(NO_3)_3]$[b]	DOJZOR	52	3.347, 3.374	2(μ_2-OR)	30.0, 34.8	+1.2
$[(LCu)_2Gd(SO_3CF_3)_2](CF_3SO_3)$[b]	LOKNOP	53	3.379, 3.384	2(μ_2-OR) (μ-O_2SOCF_3)	4.0, 6.6	+5.2
$[LCu_2Gd(OAc)_3]$[b]	GANFAD	54	3.309, 3.480	2(μ_2-OR) 2(μ-O_2CMe)	1.9	+5.0
				2(μ_2-OR) (μ-O_2CMe)	21.3	
$[(L_2Cu)_2Gd(CF_3CO_2)]$[c]	AXIHEU	55	3.314, 3.346	2(μ_2-OR) (μ-O_2CF_3)	41.1, 39.7	+3.5
$[Ni^{II}_2Gd(L)_2(NO_3)_2(MeOH)_4]$	UDEZAF	56	3.635	2(μ_2-OR)	4.5	+1.6
$[(LNi^{II}(H_2O))_2Gd(H_2O)](CF_3SO_3)_3$[c]	FUTFAC	57	3.540, 3.523	2(μ_2-OR)	18.5, 20.5	+4.8, +0.05
$[(LNi^{II})_2Gd](NO_3)$[d]	FUTFEG	57	3.321	3(μ_2-OR)	49.1	+0.9
$[L_2Ni^{II}_2Gd]$	XOFSER	58	3.314	3(μ_2-OR)	49.5	+0.8
$[(LNi^{II})_2Gd](NO_3)$[b]	IYERAF	38	3.170, 3.167	3(μ_2-OR)	90.4, 90.1	+0.4
$[(NO_3)Mn^{II}_2(L)_2(\mu$-$NO_3)Gd](NO_3)$	LUDCIX	45	3.709, 3.515	2(μ_2-OR)	3.3	+1.6
				2(μ_2-OR)(μ-NO_3)	39.9	+0.0

[a]Average distances, angles, and J values are in Å, degrees, and cm^{-1}, respectively. [b]Although the complex is not symmetric, only one exchange constant has been considered. [c]Ni^{II} cations are pentacoordinated. [d]Totally symmetric compound with two crystalographically independent molecules in the crystal structure.

$$\begin{aligned}\hat{H} = &- J_1[\hat{S}_6\hat{S}_8 + \hat{S}_7\hat{S}_9] - J_2[\hat{S}_6\hat{S}_{12} + \hat{S}_7\hat{S}_{13} + \hat{S}_8\hat{S}_{13} \\ &+ \hat{S}_9\hat{S}_{12}] - J_3[\hat{S}_6\hat{S}_{10} + \hat{S}_7\hat{S}_{11} + \hat{S}_8\hat{S}_{10} + \hat{S}_9\hat{S}_{11}] \\ &- J_4[\hat{S}_1\hat{S}_6 + \hat{S}_1\hat{S}_7 + \hat{S}_1\hat{S}_8 + \hat{S}_1\hat{S}_9 + \hat{S}_1\hat{S}_{10} + \hat{S}_1\hat{S}_{11}] \\ &- J_5[\hat{S}_2\hat{S}_6 + \hat{S}_2\hat{S}_{12} + \hat{S}_3\hat{S}_7 + \hat{S}_3\hat{S}_{13} + \hat{S}_4\hat{S}_8 + \hat{S}_4\hat{S}_{13} \\ &+ \hat{S}_5\hat{S}_9 + \hat{S}_5\hat{S}_{12}] \qquad (7)\end{aligned}$$

The calculated J values for these four complexes are collected in Table 3. Taking into account the complexity of the systems, the agreement between the theoretical results and the available experimental data is excellent. For the face-sharing complex **3** there are two different interactions, and the presence of three bridging ligands in the J_1 exchange pathway (only two for J_2) results in an antiferromagnetic coupling, associated with larger M−O···O−Gd hinge angles, as seen in the previous section. We

dx.doi.org/10.1021/ja302851n | J. Am. Chem. Soc. 2012, 134, 10532−10542

have analyzed the experimental data for trinuclear complexes (see Table 4), and even if most of them contain Ni^{II} or Cu^{II} cations, the same trend is found. Edge-sharing complexes with exchange pathways involving two bridging ligands are those with the strongest ferromagnetic interactions, while face-sharing interactions have weaker ferromagnetic couplings.

The calculated J_1 value for the butterfly $Mn^{III}_2Gd^{III}_2$ complex **4** indicates a relatively strong interaction between the Mn^{III} cations. The presence of such an interaction makes it difficult to fit the experimental data to extract accurate J values corresponding to the weak J_2–J_4 constants. Despite this fact a remarkable agreement was found with the experimental results, especially the very weak antiferromagnetic character of the J_4 interaction between the Gd^{III} centers. A more complicated case is that of the complex $[Fe^{III}_4Gd^{III}_2(\mu_4\text{-}O)_2(NO_3)_2(piv)_6(Hedte_2)]$ (**5**, H_4edte = *N*,*N*,*N*′,*N*′-tetrakis(2-hydroxyethyl)ethylenediamine, Figure 3), in which the four Fe^{III} cations are arranged in a coplanar "butterfly" conformation and each Fe_3 triangle is capped by a Gd^{III} ion. These Gd atoms are placed on opposite faces of the triangles, resulting in a very long Gd···Gd distance (7.040 Å). In this case, there is a maximum of six different exchange pathways that we have considered in our calculations, whereas the fitting of the experimental data was done with only four to avoid an overparametrization.

The signs of the calculated and experimental Fe^{III}···Fe^{III} magnetic interactions are consistent, but the sign of the Fe^{III}···Gd^{III} interactions disagree. We should keep in mind, though, that in this case the fitting procedure to obtain the Fe^{III}···Gd^{III} coupling constants is particularly difficult due to the presence of stronger Fe^{III}···Fe^{III} interactions. Both experimentally and computationally the total spin of the ground state is $S = 7$, and the first excited state has $S = 6$ (1.7 and 4.8 cm^{-1} above the ground state from experimental and calculated values, respectively). The ground-state configuration corresponds to the spin inversion relative to the highest spin case of two Fe^{III} cations that from the experimental data should be the external ones (Fe5 and Fe6), while from the calculated values they should be the inner ones (Fe3 and Fe4). The magnetic susceptibility simulated from the calculated coupling constants (Figure 4) by means the MAGPACK code[49] reproduces reasonably well the experimental behavior, taking into account the high sensitivity of the shape of the curve to the J values.

In the two previous cases, the presence of relatively strong antiferromagnetic exchange interactions between the 3d cations avoids reaching a large total spin for the complex. Thus, to have good candidates for magnetic refrigerants, it is important to avoid in the structure the presence of direct interactions between 3d cations or to have very weak antiferromagnetic interactions as in the Ni_6Gd_2·Gd complex **6**. It was not possible to accurately determine the total spin of such a system from the experimental data. The J values were calculated previously using DFT methods by some of us,[8] and this system shows a potential application in magnetic refrigeration, showing one of the highest reported changes in magnetic entropy (see Table 5). The experimental entropy value of 17.6 J kg^{-1} K^{-1} at 3 K with a change in the magnetic field $\Delta B = B_f - B_i = 50$ kG (using eq 8)[7,59] can be compared to that expected for two $S = {}^{13}/_2$ Ni_3Gd units and one $S = {}^{7}/_2$ Gd^{III} in the counteranion. $-\Delta S_m = R\ln(2S + 1)$ for each unit with total spin S; thus for the three non-interacting units we have $R[2\ln(13 + 1) + \ln(7 + 1)] = 17.9$ J kg^{-1} K^{-1}.

$$\Delta S_m(T)_{\Delta B} = \int \left[\frac{\partial M(T, B)}{\partial T}\right]_B dB \qquad (8)$$

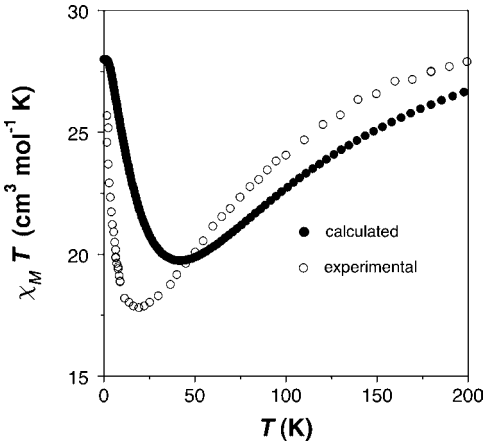

Figure 4. Magnetic susceptibility times temperature as a function of the temperature for the $Fe^{III}_4Gd^{III}_2$ complex **5**. The calculated values were obtained after the exact diagonalization of the Hamiltonian matrix using the DFT J values (see Table 3) and the experimental g value of 2.0.

Table 5. Largest-Reported Experimental Entropy Changes $-\Delta S_m$ upon Application of a Magnetic Field B at a Given Temperature for Some Polynuclear Complexes[a]

complex	$-\Delta S_m$ (J kg^{-1} K^{-1})	B (T)	T (K)	ref
Mn_{10}	13.0	7	2.2	59
Mn_{14}	25.0	7	3.8	60
Fe_{14}	17.6	7	6	61
Cr_2Gd_3	28.7	9	2.2	62
Mn_4Gd_4	19.0	7	3	63
Mn_9Gd_9	28.0	7	3	64
Mn_4Gd_6	33.7	7	3	64
Co_4Gd_6	22.3	7	3	11
Co_8Gd_8	21.4	7	3	65
Co_8Gd_4	21.1	7	3	65
Co_4Gd_6	23.6	7	3	65
Co_6Gd_8	28.6	7	3	65
Co_4Gd_2	20.0	7	3	65
Co_8Gd_2	11.8	7	3	65
Ni_6Gd_2·Gd (**6**)	17.6	5	3	8
Ni_6Gd_6	26.5	7	3	66
$Ni_{12}Gd_{36}$	36.3	7	3	67
Cu_5Gd_4	31	9	3	9
Cu_6Gd_6	23.5	7	2.3	68
Gd_2	41.6	7	1.8	69
Gd_2	20.7	5	3	70
Gd_7	23.0	7	3	71
Gd_2	23.7	7	2.4	72
Gd_4	37.7	7	2.4	72
Gd_n[b]	45.0	7	1.8	72
Gd_n[b]	47.7	7	1.8	72

[a]The solid-state compound $Gd_3Ga_5O_{12}$ usually employed in commercial applications has $-\Delta S_m = 27$ J kg^{-1} K^{-1} (at 5 T and 5 K). [b]Periodic chain structures.

The Ni_6Gd_2·Gd complex **6** is an excellent system to check if $-\Delta S_m$ can be estimated theoretically using DFT calculations. There is a well-determined X-ray crystal structure with only one complex in the unit cell, and the size of the system allows us to perform either exact diagonalization of the Hamiltonian[49] matrix or quantum Monte Carlo simulations.[73−75] Quantum Monte Carlo simulations based on the directed loop algorithm method developed by Sandvik et al.[75] were performed using the ALPS 2.0

library (dirloop_sse package).[73,74] For the temperature dependence of magnetization we considered 10^8 steps. For the susceptibility vs temperature curve, we set 10^8 steps for $T < 20$ K and 10^7 steps for simulations between 20 and 300 K. The initial 10% of steps were employed for thermalization of the system in all the calculations.

Using the DFT calculated J values (see Table 3) and performing an exact diagonalization of the Hamiltonian matrix to obtain the dependence of the magnetization on the magnetic field and temperature, and integrating eq 8 with such results using the same points that in the experimental procedure, we obtain $-\Delta S_m = 19.4$ J kg^{-1} K^{-1}, close to the experimental value of 17.6 J kg^{-1} K^{-1}. The same numerical approach was applied but now the magnetization values were independently calculated by performing a quantum Monte Carlo simulation for each temperature and magnetic field, resulting in $-\Delta S_m = 19.0$ J kg^{-1} K^{-1}. A good agreement is found when comparing the experimental dependence of $-\Delta S_m$ on temperature with those obtained from the DFT calculated J values using exact diagonalization of the Hamiltonian matrix and quantum Monte Carlo simulations (Figure 5). These results confirm that such

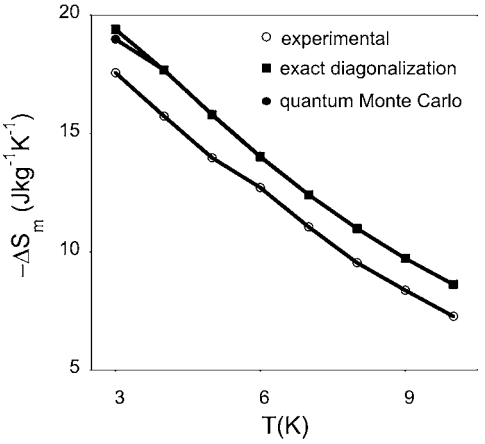

Figure 5. Dependence of $-\Delta S_m$ on the temperature for a change of the magnetic field of 5 T for the Ni_6Gd_2·Gd complex **6**.[8] Experimental values from magnetization measurements are indicated by white circles, those obtained from the DFT calculations (see Table 3) using exact diagonalization of the Hamiltonian matrix by black squares, and those obtained using quantum Monte Carlo simulations by black circles.

approximate simulations can provide accurate values and that they can be applied to larger systems for which the exact diagonalization is unfeasible, for instance the Fe_5Gd_8 complex **7**.

The last case studied is based on a very large complex, $[Fe^{III}{}_5Gd^{III}{}_8(\mu_3\text{-}OH)_{12}(L)_4(piv)_{12}(NO_3)_4(OAc)_4](H_3L)$ **7**, H_2L= *N*-butyldiethanolamine,[48] (Figure 3). The simple shape of the measured susceptibility curve and the existence of many coupling constants make it impossible to get a set of J values from the experimental data; therefore, theoretical calculations provide the only suitable method for obtaining some information about their strengths and signs. This complex is especially interesting because of its possible maximum spin $S = {}^{81}/_2$, very close to the record high spin in a Mn_{19} compound, $S = {}^{83}/_2$. However, both χT and magnetization curves tell us that the maximum values of 130.2 cm^3 K mol^{-1} and 74.4 μ_B, respectively, are far from the expected ones for the highest spin configuration, 800 cm^3 K mol^{-1} and 81 μ_B, respectively. Moreover, such susceptibility and magnetization experimental values are not consistent with each other. Thus, the χT value would suggest a total spin close to $S = {}^{30}/_2$ ($\chi T \approx 128$ cm^3 K mol^{-1}) that would point to a configuration where all the Fe^{III} spins are inverted from the highest spin state, while a magnetization closest to the experimental value (74.4 μ_B) would match a total spin $S = {}^{71}/_2$ ($M \approx 72$ μ_B) that would correspond to a situation where only the spin of one Fe^{III} ion is inverted.

The calculated J values are small when they involve Fe^{III}–Gd^{III} interactions and very small for Gd^{III}–Gd^{III} interactions, in agreement with previous computational and experimental results. The magnetic susceptibility curve obtained from the DFT J values through quantum Monte Carlo simulations[73,74] is in excellent agreement with the experimental data (see Figure 6)

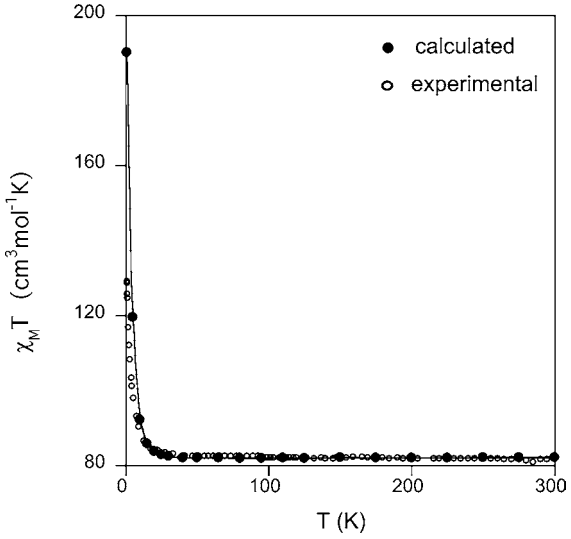

Figure 6. Temperature dependence of the χT product for the $Fe^{III}{}_5Gd^{III}{}_8$ complex **7**.[48] The calculated values were obtained from a quantum Monte Carlo simulation using the DFT J values (see Table 3) and $g = 1.96$ together with the Alps library[73,74] for the simulation, because the exact diagonalization of the Hamiltonian is not possible due to the large size of the system.

and confirms the accuracy of the employed methodology. The negative calculated J_5 value leads to a more stable single determinant configuration with $S = {}^{41}/_2$, corresponding to the spin inversion of the four corner Fe^{III} cations (Fe2, Fe3, Fe4, and Fe5 in **7**, Figure 3). Although the magnetocaloric properties of such complex were not experimentally determined, by using the DFT calculated J values (see Table 3) and performing a quantum Monte Carlo simulation for each temperature and magnetic field, we can estimate $-\Delta S_m = 7.9$ J kg^{-1} K^{-1}. This $-\Delta S_m$ value is smaller than those reported for other Gd^{III} systems in Table 5, probably due to the existence of an antiferromagnetic J_5 Fe^{III}–Gd^{III} interaction (−0.6 cm^{-1}, see Table 3). In order to check the influence of such exchange coupling constant on the $-\Delta S_m$ value, we repeated the quantum Monte Carlo simulations for two new J_5 values (−0.2 and +0.2 cm^{-1}, see Figure 7), obtaining $-\Delta S_m$ = 24.4 and 26.7 J kg^{-1} K^{-1}, respectively. This case is quite illustrative because the Fe^{III}–Gd^{III} interaction J_5 is competing with the ferromagnetic Fe^{III}–Gd^{III} interaction J_4 (+0.4 cm^{-1}) to control the sign of the spin of the four corner Fe^{III} cations (Fe2, Fe3, Fe4, and Fe5 in **7**, Figure 3). Although the two new J_5 values would lead to a ground state with the possible maximum spin $S = {}^{81}/_2$, the case with $J_5 = -0.2$ cm^{-1} has a considerable reduction of the $-\Delta S_m$ value in comparison with the $J_5 = +0.2$ cm^{-1} value

dx.doi.org/10.1021/ja302851n | J. Am. Chem. Soc. 2012, 134, 10532–10542

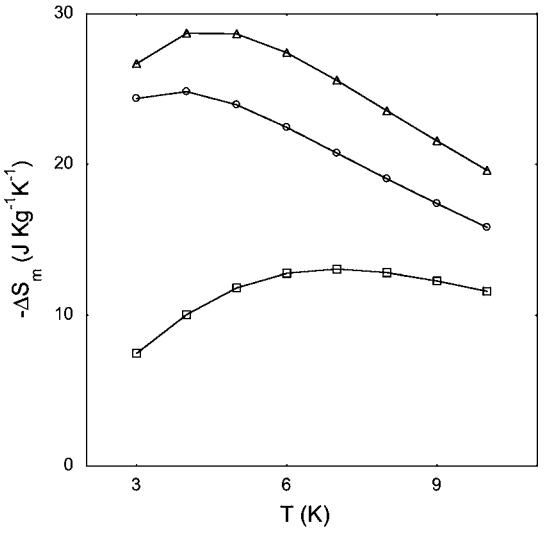

Figure 7. Dependence of $-\Delta S_m$ on the temperature for a change of the magnetic field of 5 T for the $Fe^{III}_5Gd^{III}_8$ complex **7**.[48] The calculated values were obtained from a quantum Monte Carlo simulation using the DFT J values (squares) and by replacing the calculated Fe^{III}–Gd^{III} J_5 constant of -0.6 cm^{-1} by new J values of -0.2 and $+0.2$ cm^{-1} (circles and triangles, respectively).

(see Figure 7). This is due to the presence of excited states with lower S values closer to the ground state that reduce the magnetocaloric effect. Thus, we can conclude that small changes in the calculated exchange interactions can induce relatively large changes in the $-\Delta S_m$ value and, in general, antiferromagnetic couplings should be avoided to reach the maximum magnetocaloric effect for a given system.

■ CONCLUSIONS

The magnetic properties steming from the exchange interactions in dinuclear and polynuclear 3d-Gd complexes have been studied by means of density functional methods. Large polynuclear 3d-Gd complexes showing high total spin S value, negligible magnetic anisotropy, and weak ferromagnetic couplings that favor low-lying excited states are good candidates to show large magnetocaloric effects. The first part of this work has been devoted to the analysis of the nature and the mechanism of 3d–4f exchange coupling in dinuclear complexes. If up to now most studies have focused on Cu^{II}–Gd^{III} systems, in this work we have studied Mn^{II}–Gd^{III} and Fe^{II}–Gd^{III} complexes using two different methodological approaches. The first was a numerical DFT method using the SIESTA code with a GGA functional, and in the second one we used a hybrid B3LYP functional and all-electron Gaussian basis sets, carrying out the calculations with the Gaussian09 code. The first approach was employed because it allows us to handle very large systems that are computationally inaccessible to B3LYP–Gaussian calculations.

The calculated J values for dinuclear complexes show that the numerical approach provides a good agreement with the experimental ones. In this kind of 3d metal–Gd complexes with oxo-type (e.g., alkoxo or phenoxo) bridging ligands, the key structural parameter is the M–O···O–Gd hinge angle. This dependence was already noticed for Cu^{II} and Ni^{II} complexes,[18−20] but our study shows that this geometrical parameter is also the most important one for the studied Mn^{II}–Gd^{III} and Fe^{II}–Gd^{III} complexes, regardless of whether the system has two (edge-sharing complexes) or three (face-sharing complexes) bridging ligands. It is worth remarking that changing the M–O···O–Gd hinge angle in the triply bridged systems (face-sharing complexes) also simultaneously changes the M–O–Gd bond angle, making it impossible to discern which of them is responsible for the changes in the J values. We can conclude that the presence of two bridging ligands, in comparison with those with three bridges, favors a stronger ferromagnetic coupling, especially for complexes with small M–O···O–Gd hinge angles.

The study of dinuclear systems was completed by analyzing the mechanism of the 3d-Gd exchange coupling. The results for a previously studied Cu^{II}–Gd complex,[18] as well as for the Mn^{II}–Gd^{III} and Fe^{II}–Gd^{III} complexes, show that the presence of the 5d orbitals of the Gd^{III} cations in the basis set is crucial to reproduce the experimental J values, while the 6s orbital has a negligible role from the magnetic point of view. Concerning the mechanism of the interaction, some authors have previously suggested a spin transfer from the 3d orbitals of the transition metal to the Gd 5d orbitals. However, our results for the three studied systems unequivocally show that such a mechanism should be ruled out because the 5d spin population is practically equal for the hs and ls solutions (parallel and antiparallel alignment of the spins), independently of the sign of the spin density of the 3d metal. The predominant mechanism is the spin polarization of the metal–ligand bonding electron pairs involving the formally empty 5d orbitals.

The second part of the manuscript was devoted to a computational study of demanding polynuclear 3d-Gd complexes. The use of a hybrid functional and Gaussian basis sets allowed us to calculate the exchange coupling constants of transition metal polynuclear complexes with a good accuracy. However, the inclusion of lanthanide atoms dramatically increases the required computational resources. Thus, as an alternative we have considered the use of numerical DFT calculations with a GGA functional for the study of such systems. We have studied four complexes: a $Gd^{III}Mn^{II}_2$ trinuclear complex,[45] a butterfly $Gd^{III}_2Mn^{III}_2$ system **4**,[46] the hexanuclear $Fe^{III}_4Gd^{III}_2$ compound **5**,[47] and the tridecanuclear $Fe^{III}_5Gd^{III}_8$ complex **7**.[48] The calculated J values for the studied polynuclear complexes show a remarkable agreement with the available experimental data, taking into account the complexity of these systems and the small J values involved in the exchange coupling mechanism with the Gd^{III} cations in many cases. We have employed as a test case the $Ni^{II}_6Gd^{III}_6{\cdot}Gd^{III}$ compound **6**,[8] for which the exchange coupling constants were recently reported by some of us, to check the ability of the DFT methods to reproduce the change of the entropy. This system constitutes an excellent example because it has a relatively large $-\Delta S_m$ value and it is possible to carry out the exact diagonalization of the Hamiltonian matrix to obtain the states of system using the DFT J values. This method gives a good estimate of $-\Delta S_m$ in comparison with the experimental data, and it also makes it possible to check if quantum Monte Carlo simulations can give accurate values. Such simulations using the DFT calculated J values provide a good description of the magnetic susceptibility and magnetization, in comparison with the exact diagonalization reference and the experimental data. Thus, it is possible to carry out quantum Monte Carlo simulations for very large systems in cases for which the exact diagonalization is unfeasible, as for the Fe_5Gd_8 complex (**7**). The combination of the DFT calculations with the Monte Carlo simulations is a promising predictive tool to determine the magnetic refrigeration properties and to design new improved magnetic coolers.

dx.doi.org/10.1021/ja302851n | J. Am. Chem. Soc. 2012, 134, 10532−10542

■ ASSOCIATED CONTENT

Supporting Information

Cartesian coordinates and calculated energies for the studied 3d metal−Gd complexes. This material is available free of charge via the Internet at http://pubs.acs.org.

■ AUTHOR INFORMATION

Corresponding Author

eliseo.ruiz@qi.ub.es

Notes

The authors declare no competing financial interest.

■ ACKNOWLEDGMENTS

We thank Dr. Jean-Pierre Costes for many useful discussions. The research reported here was supported by the Ministerio de Ciencia e Innovación and Generalitat de Catalunya through grants CTQ2011-23862-C02-01 and 2009SGR-1459, respectively. E.C. and S.G.C. thank Ministerio de Economía y Competividad and Ministerio de Educación, Cultura y Deporte, respectively, for a predoctoral fellowship. D.A. thanks Conicyt-Chile for a predoctoral fellowship. The authors thankfully acknowledge the computer resources, technical expertise, and assistance provided by the Barcelona Supercomputer Center.

■ REFERENCES

(1) Gheorghe, R.; Cucos, P.; Andruh, M.; Costes, J. P.; Donnadieu, B.; Shova, S. *Chem.—Eur. J.* **2006**, *12*, 187.

(2) (a) Andruh, M.; Costes, J. P.; Diaz, C.; Gao, S. *Inorg. Chem.* **2009**, *42*, 268. (b) Sessoli, R.; Powell, A. K. *Coord. Chem. Rev.* **2009**, *253*, 2328. (c) Tanase, S.; Reedijk, J. *Coord. Chem. Rev.* **2006**, *250*, 2501.

(3) Rinck, J.; Novitchi, G.; Van den Heuvel, W.; Ungur, L.; Lan, Y. H.; Wernsdorfer, W.; Anson, C. E.; Chibotaru, L. F.; Powell, A. K. *Angew. Chem., Int. Ed.* **2010**, *49*, 7583.

(4) Gatteschi, D.; Sessoli, R.; Villain, J. *Molecular Nanomagnets*; Oxford University Press: Oxford, 2006.

(5) (a) Benelli, C.; Gatteschi, D. *Chem. Rev.* **2002**, *102*, 2369. (b) Cotton, S. *Lanthanide and actinide chemistry*; John Wiley & Sons: New York, 2006.

(6) Gschneider, K. A., Jr.; Peharsky, V. K.; Tsokol, A. O. *Rep. Prog. Phys.* **2005**, *68*, 1479.

(7) Sessoli, R. *Angew. Chem., Int. Ed.* **2012**, *51*, 43.

(8) Hosoi, A.; Yukawa, Y.; Igarashi, S.; Teat, S. J.; Roubeau, O.; Evangelisti, M.; Cremades, E.; Ruiz, E.; Barrios, L. A.; Aromí, G. *Chem.—Eur. J.* **2011**, *17*, 8264.

(9) Langley, S. K.; Chilton, N. F.; Moubaraki, B.; Hooper, T.; Brechin, E. K.; Evangelisti, M.; Murray, K. S. *Chem. Sci.* **2011**, *2*, 1166.

(10) Rogez, G.; Donnio, B.; Terazzi, E.; Gallani, J.-L.; Kappler, J.-P.; Bucher, J.-P-; Drillon, M. *Adv. Mater.* **2009**, *21*, 4323.

(11) Zheng, Y. Z.; Evangelisti, M.; Winpenny, R. E. P. *Chem. Sci.* **2011**, *2*, 99.

(12) Borta, A.; Jeanneau, E.; Chumakov, Y.; Luneau, D.; Ungur, L.; Chibotaru, L. F.; Wernsdorfer, W. *New J. Chem.* **2011**, *35*, 1270.

(13) Sorace, L.; Benelli, C.; Gatteschi, D. *Chem. Soc. Rev.* **2011**, *40*, 3092.

(14) Georgopoulou, A. N.; Adam, R.; Raptopoulou, C. P.; Psycharis, V.; Ballesteros, R.; Abarca, B.; Boudalis, A. K. *Dalton Trans.* **2010**, *39*, 5020.

(15) Ferbinteanu, M.; Cimpoesu, F.; Girtu, M. A.; Enachecu, C; Tanase, S. *Inorg. Chem.* **2012**, *51*, 40.

(16) Paulovic, J.; Cimpoesu, F.; Ferbinteanu, M.; Hirao, K. *J. Am. Chem. Soc.* **2004**, *126*, 3321.

(17) Yan, F.; Chen, Z. D. *J. Phys. Chem. A* **2000**, *104*, 6295.

(18) Cirera, J.; Ruiz, E. *C. R. Chimie* **2008**, *11*, 1227.

(19) Rajaraman, G.; Totti, F.; Bencini, A.; Caneschi, A.; Sessoli, R.; Gatteschi, D. *Dalton Trans.* **2009**, 3153.

(20) Kumar Singh, S.; Kumar Tibrewal, N.; Rajaraman, G. *Dalton Trans.* **2011**, *40*, 10897.

(21) Ruiz, E.; Rodríguez-Fortea, A.; Tercero, J.; Cauchy, T.; Massobrio, C. *J. Chem. Phys.* **2005**, *123*, 074102.

(22) Ruiz, E.; Cauchy, T.; Cano, J.; Costa, R.; Tercero, J.; Alvarez, S. *J. Am. Chem. Soc.* **2008**, *130*, 7420.

(23) (a) Soler, J. M.; Artacho, E.; Gale, J. D.; García, A.; Junquera, J.; Ordejón, P.; Sánchez-Portal, D. *J. Phys.: Condens. Matter* **2002**, *14*, 2745. (b) Artacho, E.; Sánchez-Portal, D.; Ordejón, P.; García, A.; Soler, J. M. *Phys. Stat. Sol. A* **1999**, *215*, 809. (c) Artacho, E.; Anglada, E.; Diéguez, O.; Gale, J. D.; García, A.; Junquera, J.; Martin, R. M.; Ordejón, P.; Pruneda, J. M.; Sánchez-Portal, D.; Soler, J. M. *J. Phys.: Condes. Matter* **2008**, *20*, 064208.

(24) Perdew, J. P.; Burke, K.; Ernzerhof, M. *Phys. Rev. Lett.* **1996**, *77*, 3865.

(25) Kleinman, L.; Bylander, D. M. *Phys. Rev. Lett.* **1982**, *48*, 1425.

(26) Troullier, N.; Martins, J. L. *Phys. Rev. B* **1991**, *43*, 1993.

(27) Pollet, R.; Marx, D. *J. Chem. Phys.* **2007**, *126*, 181102.

(28) Douglas, M.; Kroll, N. M. *Ann. Phys.* **1974**, *82*, 89.

(29) Schäfer, A.; Huber, C.; Ahlrichs, R. *J. Chem. Phys.* **1994**, *100*, 5829.

(30) Nakajima, T.; Hirao, K. *J. Chem. Phys.* **2002**, *116*, 8270.

(31) Andruh, M.; Ramade, I.; Codjovi, E.; Guillou, O.; Kahn, O.; Trombe, J. C. *J. Am. Chem. Soc.* **1993**, *115*, 1822.

(32) Ramade, I.; Kahn, O.; Jeannin, Y.; Robert, F. *Inorg. Chem.* **1997**, *36*, 930.

(33) Benelli, C.; Caneschi, A.; Gatteschi, D.; Guillou, O.; Pardi, L. *Inorg. Chem.* **1990**, *29*, 1750.

(34) Benelli, C.; Caneschi, A.; Gatteschi, D.; Sessoli, R. *J. Appl. Phys.* **1993**, *73*, 5333.

(35) Costes, J.-P.; Clemente-Juan, J. M.; Dahan, F.; Dumestre, F.; Tuchagues, J.-P. *Inorg. Chem.* **2002**, *41*, 2886.

(36) Costes, J. P.; Dahan, F.; Dupuis, A.; Laurent, J. P. *Inorg. Chem.* **1997**, *36*, 4284.

(37) Wang, J.-H.; Yan, P.-F.; Li, G.-M.; Zhang, J.-W.; Chen, P.; Suda, M.; Einaga, Y. *Inorg. Chim. Acta* **2010**, *363*, 3706.

(38) Yamaguchi, T.; Sunatsuki, Y.; Kojima, M.; Akashi, H.; Tsuchimoto, M.; Re, N.; Osa, S.; Matsumoto, N. *Chem. Commun.* **2004**, 1048.

(39) Chen, Q.-Y.; Luo, Q.-H.; Zheng, L.-M.; Wang, Z.-L.; Chen, J.-T. *Inorg. Chem.* **2002**, *41*, 605.

(40) Costes, J.-P.; Dahan, F.; García-Tojal, J. *Chem.—Eur. J.* **2002**, *8*, 5430.

(41) Costes, J.-P.; Dahan, F.; Donnadieu, B.; Garcia-Tojal, J.; Laurent, J.-P. *Eur. J. Inorg. Chem.* **2001**, 363.

(42) Costes, J.-P.; Dahan, F.; Dupuis, A. *Inorg. Chem.* **2000**, *39*, 165.

(43) (a) Reed, A. E.; Curtiss, L. A.; Weinhold, F. *Chem. Rev.* **1988**, *88*, 899. (b) Weinhold, F., Landis, C. R. *Valency and Bonding, A Natural Bond Orbital Donor-Acceptor Perspective*; Cambridge University Press: Cambridge, 2005.

(44) (a) Cano, J.; Ruiz, E.; Alvarez, S.; Verdaguer, M. *Comments Inorg. Chem.* **1998**, *20*, 27. (b) Ruiz, E.; Cirera, J.; Alvarez, S. *Coord. Chem. Rev.* **2005**, *249*, 2649.

(45) Costes, J.-P.; García-Tojal, J.; Tuchagues, J.-P.; Vendier, L. *Eur. J. Inorg. Chem.* **2009**, 3801.

(46) Benelli, C.; Murrie, M.; Parsons, S.; Winpenny, R. E. P. *J. Chem. Soc., Dalton Trans.* **1999**, 4125.

(47) Akhtar, M. N.; Mereacre, V.; Novitchi, G.; Tuchagues, J.-P.; Anson, C. E.; Powell, A. K. *Chem.—Eur. J.* **2009**, *15*, 7278.

(48) Ako, A. M.; Mereacre, V.; Clerac, R.; Hewitt, I. J.; Lan, Y.; Anson, C. E.; Powell, A. K. *Dalton Trans.* **2007**, 5245.

(49) Borras-Almenar, J. J.; Clemente-Juan, J. M.; Coronado, E.; Tsukerblat, B. S. *J. Comput. Chem.* **2001**, *22*, 985.

(50) Bencini, A.; Benelli, C.; Caneschi, A.; Carlin, R. L.; Dei, A.; Gatteschi, D. *J. Am. Chem. Soc.* **1985**, *107*, 8128.

(51) Shiga, T.; Ohba, M.; Ōkawa, H. *Inorg. Chem.* **2004**, *43*, 4435.

(52) Bencini, A.; Benelli, C.; Caneschi, A.; Dei, A.; Gatteschi, D. *Inorg. Chem.* **1986**, *25*, 572.

(53) Costes, J.-P.; Donnadieu, B.; Gheorghe, R.; Novitchi, G.; Tuchagues, J.-P.; Vendier, L. *Eur. J. Inorg. Chem.* **2008**, 5235.

(54) Akine, S.; Matsumoto, T.; Taniguchi, T.; Nabeshima, T. *Inorg. Chem.* **2005**, *44*, 3270.
(55) Novitchi, G.; Shova, S.; Caneschi, A.; Costes, J.-P.; Gdaniec, M.; Stanica, N. *Dalton Trans.* **2004**, 1194.
(56) Shiga, T.; Ito, N.; Hidaka, A.; Ōkawa, H.; Kitagawa, S.; Ohba, M. *Inorg. Chem.* **2007**, *46*, 3492.
(57) Costes, J.-P.; Yamaguchi, T.; Kojima, M.; Vendier, L. *Inorg. Chem.* **2009**, *48*, 5555.
(58) Chandrasekhar, V.; Pandian, B. M.; Boomishankar, R.; Steiner, A.; Vittal, J. J.; Houri, A.; Clérac, R. *Inorg. Chem.* **2008**, *47*, 4918.
(59) Evangelisti, M.; Candini, A.; Ghirri, A.; Affronte, M.; Brechin, E. K.; Mcinnes, E. J. L. *Appl. Phys. Lett.* **2005**, *87*, 072504.
(60) Manoli, M.; Johnstone, R. D. L.; Parsons, S.; Murrie, M.; Affronte, M.; Evangelisti, M.; Brechin, E. K. *Angew. Chem., Int. Ed.* **2007**, *46*, 4456.
(61) Manoli, M.; Collins, A.; Parsons, S.; A. Candini, A.; Evangelisti, M.; Brechin, E. K. *J. Am. Chem. Soc.* **2008**, *130*, 11129.
(62) Birk, T.; Pedersen, K. S.; Thuesen, C. A.; Weyhermüller, T.; Schau-Magnussen, M.; Poligkos, S.; Weihe, H.; Mossin, S.; Evangelisti, M.; Bendix, J. *Inorg. Chem.* **2012**, *51*, 5435.
(63) Karotsis, G.; Evangelisti, M.; Dalgarno, S. J.; Brechin, E. K. *Angew. Chem., Int. Ed.* **2009**, *48*, 9928.
(64) Zheng, Y.-Z.; Moreno Pineda, E.; Helliwell, M.; Winpenny, R. E. P. *Chem.—Eur. J.* **2012**, *18*, 4161.
(65) Zheng, Y.-Z.; Evangelisti, M.; Tuna, F.; Winpenny, R. E. P. *J. Am. Chem. Soc.* **2012**, *134*, 1057.
(66) Zheng, Y.-Z.; Evangelisti, M.; Winpenny, R. E. P. *Angew. Chem., Int. Ed.* **2011**, *50*, 3692.
(67) Peng, J.-N.; Zhang, Q.-Q.; Kong, X.-L.; Long, L.-S.; Huang, R.-B.; Zheng, L.-S.; Zheng, Z. *Angew. Chem., Int. Ed.* **2011**, *50*, 10649.
(68) Dinca, A. S.; Ghirri, A.; Madalan, A. M.; Affronte, M.; Andruh, M. *Inorg. Chem.* **2012**, *51*, 3935.
(69) Evangelisti, M.; Roubeau, O.; Palacios, E.; Camón, A.; Hooper, T. N.; Brechin, E. K.; Alonso, J. J. *Angew. Chem., Int. Ed.* **2011**, *50*, 6606.
(70) Sedláková, L.; Hankoa, J.; Orendáčová, A.; Orendáč, M.; Zhou, C.-L.; Zhu, W.-H.; Wang, B.-W.; Wang, Z.-M.; Gao, S. *J. Alloys Compd.* **2009**, *487*, 425.
(71) Sharples, J. W.; Zheng, Y.-Z.; Tuna, F.; McInnes, E. J. L.; Collison, D. *Chem. Commun.* **2011**, *47*, 7650.
(72) Guo, F.-S.; Leng, J.-D.; Liu, J.-J.; Meng, Z.-S.; Tong, M.-L. *Inorg. Chem.* **2012**, *51*, 405.
(73) Albuquerque, A. F.; Alet, F.; Corboz, P.; Dayal, P.; Feiguin, A.; Fuchs, S.; Gamper, L.; Gull, E.; Guertler, S.; Honecker, A.; Igarashi, R.; Koerner, M.; Kozhevnikov, A.; Laeuchli, A.; Manmana, S. R.; Matsumoto, M.; McCulloch, I. P.; Michel, F.; Noack, R. M.; Pawlowski, G.; Pollet, L.; Pruschke, T.; Schollwoeck, U.; Todo, S.; Trebst, S.; Troyer, M.; Werner, P.; Wessel, S. *J. Magn. Magn. Mater.* **2007**, *310*, 1187.
(74) Bauer, B.; Carr, L. D.; Evertz, H. G.; Feiguin, A.; Freire, J.; Fuchs, S.; Gamper, L.; Gukelberger, J.; Gull, E.; Guertler, S.; Hehn, A.; Igarashi, R.; Isakov, S. V.; Koop, D.; Ma, P. N.; Mates, P.; Matsuo, H.; Parcollet, O.; Pawłowski, G.; Picon, J. D.; Pollet, L.; Santos, E.; Scarola, V. W.; Schollwöck, U.; Silva, C.; Surer, B.; Todo, S.; Trebst, S.; Troyer, M.; Wall, M. L.; Werner, P.; Wessel, S. *J. Stat. Mech.-Theory Exp.* **2011**, *2011*, P05001.
(75) Sandvik, A. W. *Phys Rev. B* **1999**, *59*, 14157.